JACS
JOURNAL OF THE AMERICAN CHEMICAL SOCIETY

ARTICLE

pubs.acs.org/JACS

Low pH Acts as Inhibitor of Membrane Damage Induced by Human Islet Amyloid Polypeptide

Lucie Khemtémourian,*[,†,‡] Elena Doménech,[†] Jacques P. F. Doux,[†] Martijn C. Koorengevel,[†] and J. Antoinette Killian[†]

[†]Biochemistry of Membranes, Bijvoet Center for Biomolecular Research, Utrecht University, Padualaan 8, 3584 CH Utrecht, The Netherlands

[‡]UPMC Univ Paris 06, UMR 7203 CNRS-UPMC-ENS, Laboratoire des Biomolécules, 4 place Jussieu, 75005, Paris, France

ABSTRACT: Human islet amyloid polypeptide (IAPP) is the major component of the amyloid deposits found in the pancreatic islets of patients with type 2 diabetes mellitus. After synthesis, IAPP is stored in the β-cell granules of the pancreas at a pH of approximately 5.5 and released into the extracellular compartment at a pH of 7.4. To gain insight into the possible consequences of pH differences for properties and membrane interaction of IAPP, we here compared the aggregational and conformational behavior of IAPP as well as IAPP−membrane interactions at pH 5.5 and pH 7.4. Our data reveal that a low pH decreases the rate of fibril formation both in solution and in the presence of membranes. We observed by CD spectroscopy that these differences in kinetics are directly linked to changes in the conformational behavior of the peptide. Mechanistically, the processes that occur at pH 5.5 and pH 7.4 appear to be similar. At both pH values, we found that the kinetic profile of IAPP fibril growth matches the kinetic profile of IAPP-induced membrane damage, and that both are characterized by a lag phase and a sigmoidal transition. Furthermore, monolayer studies as well as solid-state NMR experiments indicate that the differences in kinetics and conformational behavior as function of pH are not due to a different mode of membrane insertion. Our study suggests that a low pH prevents aggregation and membrane damage of IAPP in the secretory granules, most likely by affecting the ionization properties of the peptide.

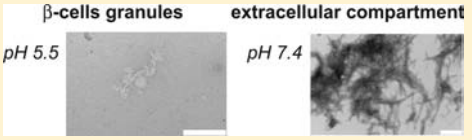

INTRODUCTION

The formation of protein amyloid deposits is associated with major human diseases including Alzheimer's disease, Parkinson's disease, the spongiforme encephalopathy, and type 2 diabetes mellitus.[1−3] Type 2 diabetes mellitus (DM2) is characterized metabolically by defects in both insulin secretion and insulin action, resulting in hyperglycemia, and is characterized histopathologically by the presence of fibrillar amyloid deposits in the pancreatic islets of Langerhans (islet amyloid).[4] The presence of these amyloid deposits has been linked to death of the insulin-producing islet β-cells.[4] Islet amyloid polypeptide (IAPP), a 37 amino acid peptide, is the major constituent of the amyloid deposits found in type 2 diabetic patients. IAPP and insulin are coproduced and cosecreted together by the pancreatic islet β-cells and have complementary hormone activities. In its soluble form, monomeric IAPP is involved in the regulation of glucose homeostasis, in gastric emptying, and in other cellular processes.[5−8]

It has been found that in vivo IAPP remains soluble and is safely stored in secretory vesicles at millimolar concentrations, while in vitro IAPP forms amyloid fibrils in a few hours at very low concentrations (as low as 1 μM). In contrast, progression of DM2 takes many years. Therefore, it is likely that other factors act as chaperones to stabilize IAPP in a nontoxic form. The in vivo environment includes factors like pH values, ionic strength, and metal ion and protein components such as insulin, proinsulin, and proIAPP, which must play a critical role in preventing IAPP misfolding into fibrillar amyloid. Indeed, it was shown that insulin inhibits IAPP fibril formation in vitro.[9−15] Recent studies show that zinc, which is found at millimolar concentrations in the secretory granule, significantly inhibits IAPP amyloid fibrillogenesis at concentrations similar to those found in the extracellular environment.[16,17] Another study suggests that the IAPP precursors, prohIAPP$_{1-67}$ and prohIAPP$_{1-48}$, prevent aggregation and membrane damage of mature IAPP in early stages of its biosynthesis and intracellular transport.[18]

IAPP contains a single histidine at position 18, which has a charge that depends on pH in a physiological pH range. Consequently, it is feasible that fibril formation and membrane interactions of IAPP are dependent on pH. This would be interesting from a biological point of view, because mature IAPP is stored in the β-cell granules of the pancreas at a pH of approximately 5.5 and released into the extracellular compartment, which has a pH of 7.4. Studies have shown that aggregation of IAPP in solution is considerably slower at a low pH of 4.0 than at a pH of 8.8 and that the fibril morphology is affected by a very low pH of 2.4.[19,20] On the other hand, studies on IAPP have shown that membranes can play an active role in amyloid formation. For example, it was shown that the presence of phospholipid membranes can promote IAPP aggregation, in particular when these membranes contain negatively charged lipids.[21] However, to our knowledge,

Received: May 31, 2011
Published: August 26, 2011

no reports have been published so far on the interaction between membranes and IAPP at a lower pH of approximately 5.5, despite its potential biological relevance.

To gain more insight into the possible physiological importance of pH, we examined the aggregational and conformational behavior of IAPP at pH 5.5 as compared to pH 7.4 in the absence and presence of lipid bilayers. In addition, we monitored the effect of pH on membrane integrity and on kinetics and extent of membrane insertion of IAPP. For these studies, we used mixtures of the zwitterionic lipid phosphatidylcholine (PC) and the anionic lipid phosphatidylserine (PS) in a 7:3 ratio to mimic the membranes of pancreatic islet cells.[22] We find that a low pH has significant consequences for the properties and membrane interaction of the peptide.

MATERIALS AND METHODS

Materials. IAPP was obtained from Bachem AG. Its amino acid sequence is: KCNTATCATQRLANFLVHSSNNFGAILSSTNVGSNTY. 1,2-Dioleoyl-*sn*-glycero-3-phosphocholine (DOPC) and 1,2-dioleoyl-*sn*-glycero-3-phospho-L-serine (DOPS), chain perdeuterated 1-palmitoyl-2-oleoyl-*sn*-glycero-3-phosphocholine (POPC-d_{31}), and 1-palmitoyl-2-oleoyl-*sn*-glycero-3-phospho-L-serine (POPS) were obtained from Avanti Polar Lipids. Thioflavin T (ThT) was obtained from Sigma.

Preparation of Peptide Samples. Peptide stock solutions were prepared as described previously.[23] Briefly, peptides were dissolved at a concentration of 1 mM in hexafluoro-isopropanol (HFIP) and incubated for at least 1 h. Next, HFIP was evaporated followed by vacuum desiccation for at least 30 min. For the ThT-fluorescence, the membrane leakage, and the microscopy experiments, the peptide film was then dissolved in DMSO to a final peptide concentration of 0.2 mM. For those experiments, we used the same concentration of DMSO (2.5% in the final volume), and hence we were able to compare for those experiments the shape of the curve and the lag time. For the CD experiments, the resulting peptide film was solubilized by addition of a dispersion of LUVs. For the NMR experiments, the resulting peptide film was solubilized by addition of the mixture of lipids in chloroform.

Preparation of Large Unilamellar Vesicles (LUVs). The LUVs were composed of a mixture of DOPC/DOPS in a 7:3 molar ratio. Stock solutions of DOPC and DOPS in chloroform at concentrations of 20−30 mM were mixed in a glass tube. The solvent was evaporated with dry nitrogen gas yielding a lipid film that was subsequently kept in a vacuum desiccator for 20 min. Lipid films were hydrated in 10 mM Tris·HCl, 100 mM NaCl buffer (pH 7.4 and pH 5.5) during at least 30 min, at a lipid concentration of 10 mM. The lipid suspensions were subjected to 10 freeze−thaw cycles, at temperatures of approximately −80 and 40 °C, respectively, and subsequently extruded 10 times through 0.2 μm-pore size filters (Anotop 10, Whatman, Maidstone, U.K.). The phospholipid content of lipid stock solutions and vesicle preparations was determined as inorganic phosphate according to Rouser.[24] Calcein-containing LUVs were made using the same protocol as previously, except for the following adaptations. The buffer for hydration of the lipid film was replaced by a buffer containing 70 mM calcein and 10 mM Tris·HCl (pH 7.4 and pH 5.5). Free calcein was separated from the calcein-filled LUVs using size-exclusion column chromatography (Sephadex G-50 fine) and elution with a 10 mM Tris·HCl, 100 mM NaCl buffer (pH 7.4 and pH 5.5).

Electron Microscopy. Peptides and LUVs were incubated under the same conditions as in the Thioflavin T assay. Aliquots (20 μL) of this mixture were adsorbed onto glow-discharged carbon-coated 300-mesh copper grids for 2 min. Grids were then blotted and dried. Grids were negatively stained for 45 s on 2% uranyl acetate, blotted, and dried. Grids were examined using a Technai 12 electron microscope operating at 120 kV.

Thioflavin T Assay. The kinetics of fibril formation was measured using the fluorescence intensity increase upon binding of the fluorescent dye Thioflavin T (ThT) to fibrils. A plate reader (Spectrafluor; Tecan) and standard 96-wells flat-bottom black microtiter plates in combination with a 430 nm excitation filter and a 535 nm emission filter were used as described previously. The ThT assay in the presence of membranes was started by adding 5 μL of a 0.2 mM IAPP in DMSO to 195 μL of a mixture of 10 μM ThT, LUVs (43 μM lipids), and 10 mM Tris/HCl, 100 mM NaCl (pH 7.4 or pH 5.5). The ThT assay in solution was performed using the same method but without the addition of the LUVs. The microtiter plate was shaken for 10 s directly after addition of all components, but not during the measurement. The ThT assay were performed three times, each in triplicate, on different days, using different IAPP stock solutions.

Membrane Permeability Experiments. A plate reader (Spectrafluor, Tecan, Salzburg, Austria) was used to perform leakage experiments in standard 96-wells transparent microtiter plates. The leakage assay was started by adding 5 μL of a 0.2 mM IAPP stock solution in DMSO to 195 μL of a mixture of calcein containing LUVs (43 μM lipids) and 10 mM Tris/HCl, 100 mM NaCl (pH 7.4 or pH 5.5). The DMSO concentration of all samples was matched to 2.5% (v/v). Directly after addition of all components, the microtiter plate was shaken for 10 s using the shaking function of the plate reader. The plate was not shaken during the measurement. Fluorescence was measured from the top, every 5 min, using a 485 nm excitation filter and a 535 nm emission filter. The temperature during the measurement was 28 ± 3 °C. The maximum leakage at the end of each measurement was determined by adding 1 μL of 10% Triton X-100 to a final concentration of 0.05% (v/v). The release of fluorescent dye was calculated according to eq 1:

$$L(t) = (F_t - F_0)/(F_{100} - F_0) \quad (1)$$

$L(t)$ is the fraction of dye released (normalized membrane leakage), F_t is the measured fluorescence intensity, and F_0 and F_{100} are the fluorescence intensities at times t = 0 and after addition of Triton X-100, respectively. The membrane leakage assay was performed three times, each in triplicate, on different days, using different IAPP stock solutions

CD Spectroscopy. CD spectra were measured on a Jasco 810 spectropolarimeter (Jasco Inc., Easton, MD) over the wavelength range 190−270 nm. Measurements were carried out in cells of 0.1 cm path length at room temperature in aqueous solution (10 mM phosphate buffer) at pH 7.4 and at pH 5.5 and in DOPC/DOPS (7:3) LUVs in 10 mM phosphate buffer (pH 7.4 and pH 5.5). Measurements were taken every 0.2 nm at a scan rate of 20 nm/min. Each spectrum reported is the average of five scans. Peptide concentrations were 25 μM in the absence and in the presence of lipids (peptide:lipid ratio 1:20).

Sample Preparation for NMR Experiments. Mixtures of POPC-$^2H_{31}$ and POPS (ratio 7:3) were codissolved in chloroform and evaporated under vacuum. The residual lipid film was hydrated in Tris-HCl, 100 mM NaCl buffer (pH 7.4 or pH 5.5). The solution was subjected to 10 freeze−thaw cycles, at temperatures of approximately −80 and 40 °C, to homogenize the size of the multilamellar vesicules. For the samples containing IAPP, the lipid solution was added to the film of peptide at the beginning of the vesicle preparation. A total peptide:lipid ratio of 1:20 was used. Samples were transferred into a 4 mm NMR rotor (100 μL) for wide line experiments.

NMR Experiments. NMR experiments were carried out on a Bruker Advance 500 MHz NMR spectrometer. ^{2}H NMR experiments on deuterated lipids were performed at 76.78 MHz using a quadrupolar echo sequence.[25] Typical acquisition parameters were as follows: a 2.5 μs 90° pulse, an echo delay of 50 μs, a recycling delay of 1.5 s, a 500 kHz spectral width, and 20 000 scans. A line broadening of 100−200 Hz was applied prior to Fourier transformation. The temperature was regulated

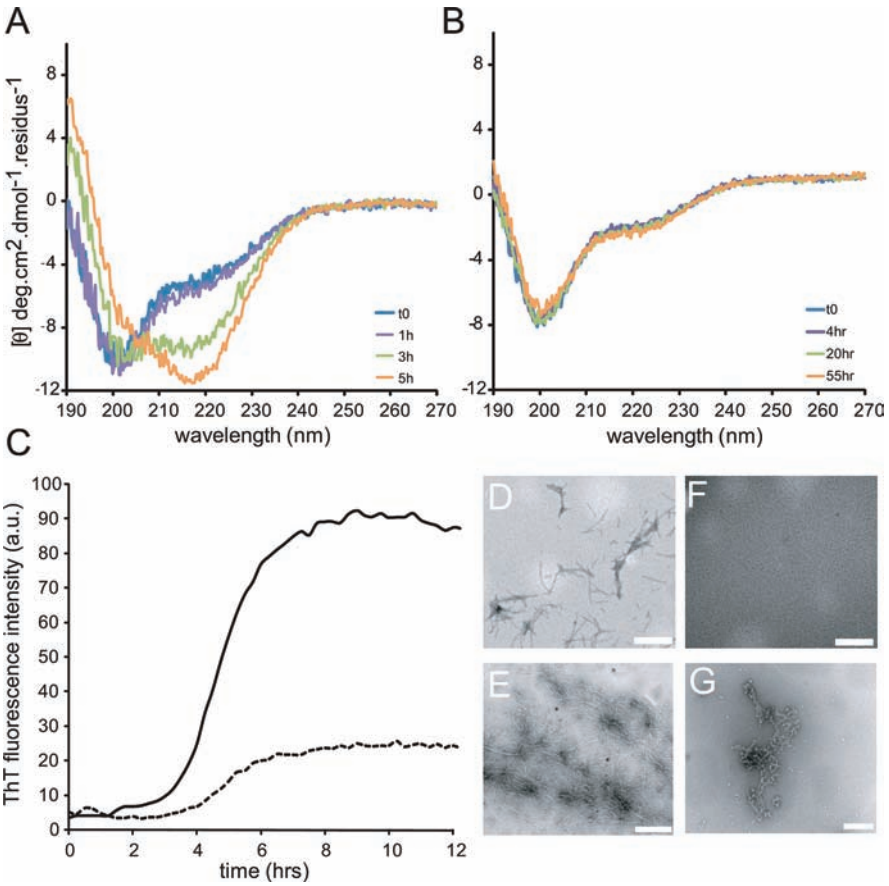

Figure 1. CD spectra of IAPP at 25 μM in solution, measured as function of time at pH 7.4 (A) and at pH 5.5 (B). (C) ThT fluorescence of fibril formation of IAPP at 5 μM in solution at pH 7.4 (—) and at pH 5.5 (- - -). Negatively stained microscopy images of IAPP at 5 μM at pH 7.4 after incubation of 4 and 24 h (respectively, D, scale bars 200 nm, and E, scale bars 500 nm) and at pH 5.5 after incubation of 4 and 24 h (F and G, respectively, scale bars 200 nm).

at 25 ± 1 °C. Proton-decoupled ^{31}P NMR experiments were performed at 202.47 MHz using a Hahn-echo sequence.[26,27] Typical acquisition parameters were as follows: a 5 μs 90° pulse, an echo delay of 20 μs, a recycling delay of 1 s, a 250 ppm spectral width, and 3000−4000 scans.

RESULTS AND DISCUSSION

Low pH Inhibits Fibril Formation of IAPP in Solution. It has been shown that the conformation of IAPP in solution at neutral pH changes within a few hours from random coil to β-sheet, indicative of amyloid fibrils.[28] We first performed CD measurements to analyze the conformational changes of the peptide after a few hours of incubation in the absence of membranes at pH 5.5 and pH 7.4. The CD spectra of IAPP, freshly dissolved in 10 mM phosphate buffer at 25 μM, are identical at pH 5.5 and pH 7.4, displaying a peak with negative ellipticity at 200 nm that is characteristic of a random coil conformation (Figure 1A,B). However, after a few hours of incubation, IAPP at pH 7.4 adopts a β-sheet structure, while IAPP at pH 5.5 retains its random coil configuration. The CD signal of IAPP at pH 5.5 remains stable for at least 2 days and shows no evidence of β-sheet structure, indicative of amyloid fibril formation.

Next, to examine whether indeed the formation of IAPP amyloid fibrils is hampered at low pH, we used the complementary approach of measuring fluorescence intensity changes upon binding of the amyloid specific dye Thioflavin T (ThT), which is a commonly used method to detect amyloid fibrils.[29] Using this method, the kinetics of fibril formation was followed at pH 5.5 and pH 7.4 and at a peptide concentration of 5 μM at 25 °C. Figure 1C shows typical curves obtained for IAPP at pH 7.4 and pH 5.5. The curves are S-shaped, which is a well-known characteristic of amyloid fibril formation.[30] At pH 7.4, the lag time is approximately 3−4 h, but at pH 5.5 a longer lag time (approximately 5−6 h) is observed accompanied by a reduced final fluorescence intensity. This reduction of fluorescence intensity should not necessarily be interpreted in terms of the amount of amyloid formed. Indeed, the changes in the binding constant or the quantum yield of the dye can also contribute to any observed differences. Thus, it is critical to assay fibril formation by an independent method, such as for example transmission electron microscopy (TEM). Figure 1D,E shows that IAPP forms fibrils at pH 7.4 within a few hours of incubation in buffer. The fibrils exhibit the typical morphology of amyloid fibrils with widths between 10 and 15 nm. For IAPP at pH 5.5 at the same concentration, no fibrils are observed within 4 h of incubation, while 24 h of incubation is required to obtain some fibrils (Figure 1F,G). However, the morphology of the fibrils of IAPP at pH 5.5 is different from the one at pH 7.4. The population of IAPP fibrillar assemblies at pH 5.5 consist of somewhat amorphous, short fibrils that, contrary to IAPP at pH 7.4, do not appear to have a strong propensity to cluster into a more or less regular pattern. Our results are consistent with

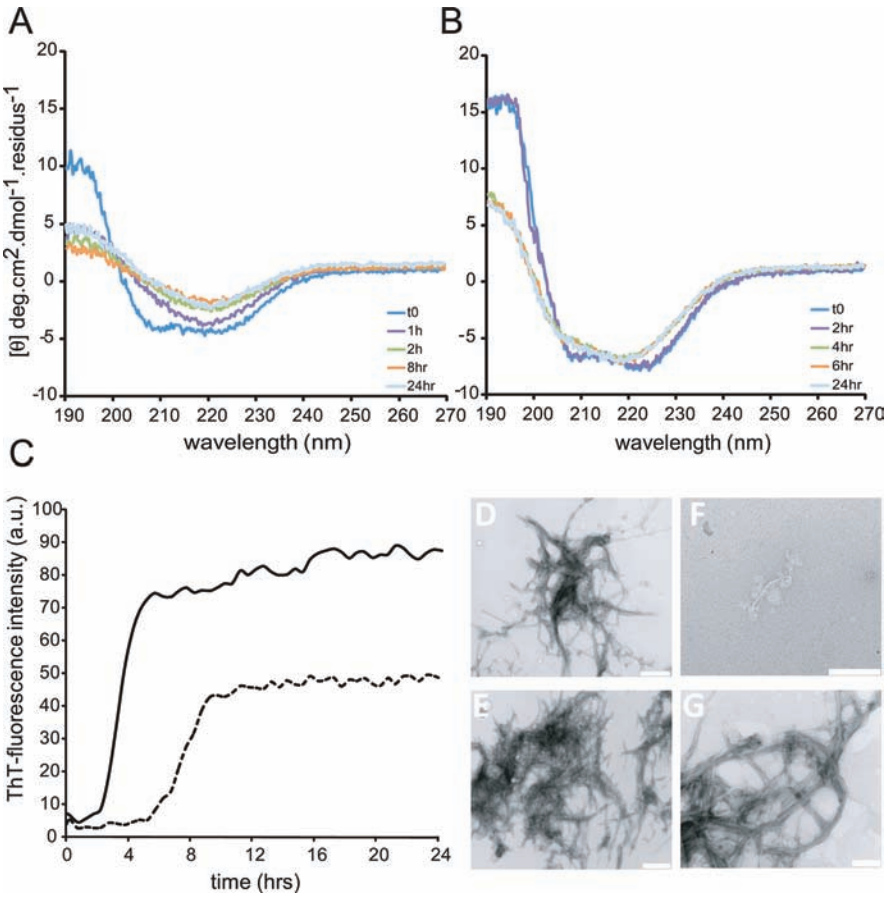

Figure 2. CD spectra of IAPP at 25 μM in the presence of DOPC/DOPS 7:3 LUV (ratio peptide:lipid 1:20), measured as function of time at pH 7.4 (A) and at pH 5.5 (B). (C) ThT fluorescence of fibril formation of IAPP at 5 μM in the presence of DOPC/DOPS 7:3 LUV at pH 7.4 (—) and at pH 5.5 (- - -). Negatively stained microscopy images of IAPP in the presence of DOPC/DOPS 7:3 LUV at pH 7.4 after incubation of 4 and 24 h (respectively, D, scale bars 500 nm, and E, scale bars 1 μm) and at pH 5.5 after incubation of 4 and 24 h (respectively, F, scale bars 500 nm, and G, scale bars 200 nm).

previous studies of IAPP in solution where much lower pH values were used (respectively, pH 2.4 and 4.0).[19,20]

The Membrane Catalyzes fibril Formation at Neutral and at Low pH. Next, the same experiments were carried out in the presence of large unilamellar vesicles (LUVs) composed of DOPC/DOPS in a molar ratio of 7:3. It was already shown that at pH 7.4 and upon interaction with membranes IAPP adopts an α-helical conformation, which in time undergoes a transition to β-sheet.[31] The spectrum in Figure 2A confirms this behavior, and Figure 2B shows that a similar transition occurs at pH 5.5. Immediately upon addition to the DOPC/DOPS LUVs, the CD spectra of IAPP at pH 5.5 and pH 7.4 are identical, displaying negative ellipticity at 208 and 222 nm, characteristic of an α-helical backbone structure (Figure 2A,B), and in time they convert to β-structure. However, there is a difference in kinetics. After a short time of incubation (1 h), IAPP already adopts some β-sheet structure at pH 7.4, while after 2 h of incubation the spectrum for IAPP at pH 5.5 is still unchanged. In addition, a slight difference in intensity is noticed, indicating that the proportion of α-helical structure is somewhat larger at pH 5.5 than at pH 7.4. The fact that IAPP adopts a β-sheet structure at pH 5.5 in the presence of membranes may signify that also in this case IAPP can form fibrils. ThT-fluorescence experiments in the presence of DOPC/DOPS membranes (Figure 2C) suggest that indeed fibrils are formed, and that the kinetics of fibril formation at pH 5.5 (lag time of 5—6 h) are slower than that at pH 7.4 (lag time of approximately 2 h), in agreement with the CD data. Figure 2C also shows that the final fluorescence intensity is reduced at low pH. Consistent with this, we observed by using TEM the formation of fibrils for IAPP at pH 7.4 after 4 h incubation, while for IAPP at pH 5.5, no fibrils were observed after the same time of incubation (Figure 2F). However, after 24 h also in this case fibrils were obtained (Figure 2G). In both cases (pH 7.4 and pH 5.5), the fibrils exhibited the typical morphology of amyloid fibrils. Thus, our results demonstrate that membranes catalyze fibril formation of IAPP at pH 7.4, in agreement with previous results,[21] as well as at pH 5.5.

IAPP—Membrane Damage Is Linked to Fibril Formation and Is Strongly pH-Dependent. Previously, for IAPP a correlation was found between fibril formation and peptide-induced membrane damage at pH 7.4.[23] It was postulated that fibril formation of IAPP at the membrane surface causes IAPP-induced membrane damage. If these processes of fibril formation and membrane damage are indeed causally related, we would expect that at pH 5.5 the process of membrane damage would be slower than that at pH 7.4. Membrane damage was assayed quantitatively by analyzing the extent of leakage of a fluorescent dye (calcein) from large unilamellar vesicles (LUVs), which is an established membrane leakage assay to study membrane interactions of amyloidogenic peptides.[32,33] Figure 3A shows that in DOPC/DOPS LUVs, IAPP is able to induce after 24 h about 80% of membrane leakage at pH 7.4 and around 60% at pH 5.5.

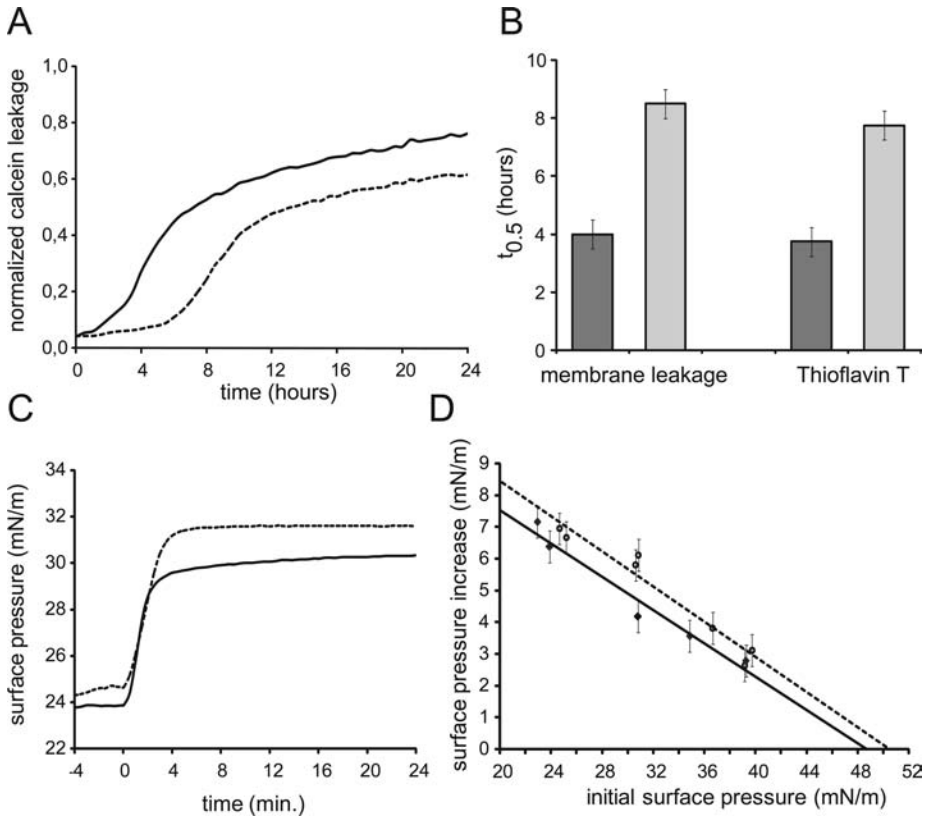

Figure 3. (A) Kinetics of membrane permeabilization by 5 μM hIAPP at pH 7.4 (—) and pH 5.5 (- - -). The peptide was added to the calcein containing DOPC/DOPS (7:3) LUVs at $t = 0$. The maximum leakage, after complete disruption of all vesicles by Triton, was set at 1. (B) The average midpoints ($t_{0.5}$) of the sigmoidal transitions for both ThT fluorescence and membrane leakage are shown for experiments at pH 7.4 (dark gray) and at pH 5.5 (light gray), for three independent experiments, each performed in triplicate, on different days, using different IAPP stock solutions. The error bars indicate the standard deviation. (C) Surface pressure profile after injecting a sample of IAPP at pH 7.4 (—) and at pH 5.5 (- - -) in a monolayer of DOPC/DOPS (7:3). The peptides were injected into the stirred subphase at $t = 0$ min. The final peptide concentration was 1 μM. (D) Surface pressure increase induced by the interaction of freshly dissolved IAPP at pH 7.4 (—) and at pH 5.5 (- - -) with DOPC/DOPS (7:3) monolayers as a function of the initial surface pressure. The straight lines were obtained by linear regression.

In addition, it shows that at pH 7.4 the lag time is shorter (~2 h) than that at pH 5.5 (~6 h). Comparison of these kinetic profiles of membrane leakage with those of fibril formation (Figure 2C) shows that they both are characterized by a lag phase and a sigmoidal transition. Importantly, the lag times in both processes overlap, as indicated by the similar values for the midpoints ($t_{0.5}$) of the sigmoidal transitions (Figure 3B), suggesting a direct correlation between the processes of membrane leakage and fibril formation.

IAPP Inserts Efficiently into Lipid Monolayer Both at Neutral and at Low pH. Our data demonstrate that the membrane leakage is slower at pH 5.5 than at pH 7.4. A possible hypothesis is that this observed difference in IAPP—membrane damage at pH 5.5 and pH 7.4 is caused by differences in membrane insertion. To study the insertion of peptide in lipid membranes, we performed monolayer experiments at both pH values. Insertion of peptide into a monolayer of phospholipids at the air/water interface can be monitored as an increase in the surface pressure of the monolayer.[34] Injection of a solution of IAPP in the aqueous subphase below a DOPC/DOPS (7:3) monolayer results in a fast increase in the surface pressure, followed by a plateau starting at approximately 5 min after addition of peptide, both at pH 7.4 and at pH 5.5 (Figure 3C). After 20 min and at initial surface pressures of approximately 24 mN/m, the increase in surface pressure induced by insertion of IAPP at pH 7.4 is 6.5 ± 0.5 mN/m, as compared to an increase of 6.9 ± 0.5 mN/m for IAPP at pH 5.5. At this starting surface pressure, IAPP insertion is about the same at both pH values. Next, we analyzed the surface pressure increase as a function of initial surface pressure. The data from Figure 3D indicate that the extrapolated "limiting surface pressure" is very high and roughly the same for IAPP at pH 5.5 (50.5 ± 1.0 mN/m) and at pH 7.4 (48.7 ± 1.0 mN/m). In both cases, the limiting surface pressure is significantly higher than the surface pressures that correspond to the packing density in lipids in biological membranes, between 31 and 35 mN/m,[35] indicating that also in vivo IAPP can insert efficiently into membranes at pH 5.5 and pH 7.4. Altogether, our monolayer data demonstrate that the differences we observed at different pH in the membrane leakage experiments are not due to differences in the kinetics or extent of peptide membrane insertion.

A Strong Effect of IAPP on Lipid Order Is Observed Both at Low and at Neutral pH. To obtain more details about the mode of membrane insertion of IAPP and the protein/lipid interactions involved, we determined the influence of addition of IAPP on lipid order by ^{2}H NMR and ^{31}P NMR. The peptide was incorporated into multilamellar vesicles of perdeuterated POPC-$^{2}H_{31}$/POPS at a 1/20 peptide/lipid molar ratio. Figure 4A and D presents the ^{2}H NMR spectra of POPC-$^{2}H_{31}$/POPS bilayer dispersions without peptide at pH 7.4 and at pH 5.5, respectively.

dx.doi.org/10.1021/ja205007j |J. Am. Chem. Soc. 2011, 133, 15598–15604

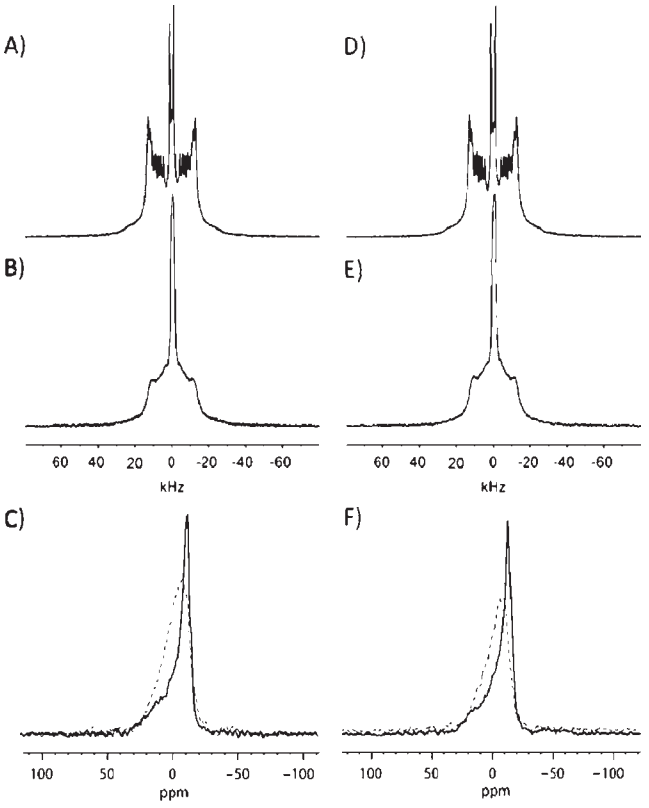

Figure 4. ^{2}H NMR spectra of IAPP on fluid POPC-$^{2}H_{31}$/POPS multilamellar vesicles at 25 °C: (A) and (D) without IAPP at pH 7.4 and at pH 5.5, respectively; (B) and (F) in the presence of IAPP (ratio peptide:lipid 1:20) at pH 7.4 and at pH 5.5, respectively. Wideline proton-decoupled ^{31}P NMR spectra of POPC-$^{2}H_{31}$/POPS multilamellar vesicles at 25 °C at pH 7.4 (C) and at pH 5.5 (F) in the absence of peptide (—) and in the presence of IAPP (- - -).

At both pH values, we observe the typical spectrum with many resolved splittings that is characteristic of a lamellar fluid phase.[36] The smallest splitting, corresponding to the methyl groups at the end of the acyl chains, is about 3 kHz and is reporting the lipid order in the membrane center. The largest one, corresponding to the CD_2 groups closest to the glycerol backbone, is approximately 26 kHz and is giving information about lipid order near the interface. Intermediate labeled positions show splittings between 9 and 26 kHz. The variation of quadrupolar splitting with labeled carbon positions depicts the well-known gradient of internal membrane ordering.[37] Addition of IAPP leads to notable changes independent of the pH (Figure 4B—E). The quadrupolar splittings for each position are now ill defined and have a longer width distribution. Two possible explanations are (1) that after addition of the peptide the vesicles become smaller with a heterogeneous size distribution and (2) that IAPP—membrane insertion perturbs the lipid acyl chain order and the membrane dynamics. To gain more insight into these possibilities, ^{31}P NMR was used to report on IAPP—membrane interactions from the point of view of the membrane surface. Figure 4C and F shows classical axially symmetric spectra for the POPC-$^{2}H_{31}$/POPS system, in the absence (—) and presence (- - -) of IAPP. Spectra in the absence of IAPP are the superposition of two subspectra originating from the phosphorus nuclei of DOPC and DOPS. Because of the different headgroup structures of the two lipids, each subspectrum shows a slightly different residual chemical shift anisotropy.[38] Spectra in the presence of IAPP are less intense but clearly broader with more averaging of the chemical shift anisotropy independently of the pH. This suggests that, similar to the acyl chains, either the headgroups are strongly affected by the presence of the peptide or the vesicles become smaller after addition of the peptide. The latter interpretation was supported by DLS experiments on POPC/POPS at pH 7.4 and pH 5.5 to measure the size of the vesicles before and after the addition of the peptide (data not shown). Heterogeneous sizes with a diameter of around 400—800 nm were mostly detected in the absence of peptide. On addition of IAPP at both pH values, the system seemed converted into objects with a diameter between 50 and 200 nm (most likely corresponding to small lipid vesicles) and objects of approximately 3000 nm (most likely corresponding to the peptide aggregates). Thus, our NMR experiments support a strong interaction of the peptides with the lipid vesicles both at low and at neutral pH, but due to the size reduction of the vesicles, they do not allow one to draw conclusions on effects of headgroup or lipid order. Altogether our data show that the kinetics of IAPP-induced membrane damage and fibril formation are strongly dependent on the pH, whereas IAPP—membrane insertion itself is not.

SUMMARIZING CONCLUSIONS

Two important conclusions can be drawn from the results of this study. First, our results show that membranes catalyze fibril formation of IAPP at pH 7.4 as well as at pH 5.5 and that the kinetics of fibril formation and the kinetics of membrane damage are related at both pH values. Previously, such a correlation was found at pH 7.4, and it was postulated that at least under these specific conditions, it is the growth of IAPP fibrils at the membrane surface rather than the formation of oligomeric species that causes IAPP-induced membrane damage.[23] The tendency of amyloidogenic peptides to fibrillate on the surface of lipid vesicles, and simultaneously damage the lipid bilayer, has also been observed using molecular dynamics simulations.[39] Recently, the group of Lashuel showed that Aβ toxicity is mediated by the process of fibril formation and not by a specific Aβ species.[40] Therefore, we speculate that this may be a general mechanism for causing membrane disruption by amyloid forming proteins. The second important conclusion from the present study is that the kinetics of fibril formation and of membrane damage are strongly pH-dependent and can be directly linked to the conformational behavior. This is in contrast to the IAPP—membrane interactions as analyzed by monolayer insertion studies and by ^{31}P NMR and ^{2}H NMR, which show no pH dependence. Because the histidine residue at position 18 is the only residue that titrates over the pH range, we can conclude (i) that the ionization state of this histidine significantly affects the kinetics of conformational changes and concomitant fibril formation and (ii) that this is directly related to the kinetics of membrane damage. This is consistent with a result from a recent study on the N-terminal part of the peptide ($IAPP_{1-19}$), which showed that the protonation of the histidine causes a change in its membrane binding topology.[41] All of our studies show that fibril formation and membrane damage occur at a slower rate at pH 5.5 than at pH 7.4. Because IAPP is stored in the β-cell granules at an acidic pH and released into the extracellular compartment at a pH of 7.4, we thus may assume that the lower pH of the granules protects IAPP from fibril formation. Although the differences we observed at low pH are not large as compared to the results at

physiological pH, it is very well possible that in vivo they play a more significant role. In addition, factors other than pH changes (for example, ionic strength, concentration of metal ions, or the presence of insulin) may contribute significantly to amyloid formation in vivo. Indeed, some studies showed that zinc has an overall inhibitory effect on IAPP fibril formation[16,17] and that insulin decreases the ability of IAPP to permeabilize membranes.[15]

AUTHOR INFORMATION

Corresponding Author
lucie.khemtemourian@upmc.fr

ACKNOWLEDGMENT

We thank Hans Meeldijk for his help in the electron microscopy experiments. This study was supported by the European Commission through a Marie Curie Postdoctoral fellowship (MCA-EIF). J.P.F.D. was supported by The Netherlands Organization for Scientific Research (NWO).

REFERENCES

(1) Chiti, F.; Dobson, C. M. *Annu. Rev. Biochem.* **2006**, *75*, 333–66.
(2) Selkoe, D. J. *Nature* **2003**, *426*, 900–904.
(3) Sipe, J. D. *Crit. Rev. Clin. Lab. Sci.* **1994**, *31*, 325–54.
(4) Höppener, J. W. M.; Ahrén, B.; Lips, C. J. *N. Engl. J. Med.* **2000**, *343*, 411–9.
(5) Karlsson, E. *Int. J. Mol. Med.* **1999**, *3*, 577–84.
(6) Akesson, B.; Panagiotidis, G.; Westermark, P.; Lundquist, I. *Regul. Pept.* **2003**, *111*, 55–60.
(7) Reda, T. K.; Geliebter, A.; Pi-Sunyer, F. X. *Obes. Res.* **2002**, *10*, 1087–91.
(8) Rushing, P. A.; Hagan, M. M.; Seeley, R. J.; Lutz, T. A.; D'Alessio, D. A.; Air, E. L.; Woods, S. C. *Endocrinology* **2001**, *142*, 5035.
(9) Westermark, P.; Li, Z. C.; Westermark, G. T.; Leckstrom, A.; Steiner, D. F. *FEBS Lett.* **1996**, *379*, 203–206.
(10) Jaikaran, E. T.; Nilsson, M. R.; Clark, A. *Biochem. J.* **2004**, *377*, 709–16.
(11) Gilead, S.; Wolfenson, H.; Gazit, E. *Angew. Chem., Int. Ed.* **2006**, *45*, 6476–6480.
(12) Larson, J. L.; Miranker, A. D. *J. Mol. Biol.* **2004**, *335*, 221–31.
(13) Kudva, Y. C.; Mueske, C.; Butler, P. C.; Eberhardt, N. L. *Biochem. J.* **1998**, *331*, 809–813.
(14) Knight, J. D.; Williamson, J. A.; Miranker, A. D. *Protein Sci.* **2008**, *17*, 1850–1856.
(15) Brender, J. R.; Lee, E. L.; Hartman, K.; Wong, P. T.; Ramamoorthy, A.; Steel, D. G.; Gafni, A. *Biophys. J.* **2011**, *100*, 685–92.
(16) Brender, J. R.; Hartman, K.; Nanga, R. P. R.; Popovych, N.; Bea, R. D.; Vivekanandan, S.; Marsh, E. N. G.; Ramamoorthy, A. *J. Am. Chem. Soc.* **2010**, *132*, 8973–8983.
(17) Salamekh, S.; Brender, J. R.; Hyung, S. J.; Nanga, R. P.; Vivekanandan, S.; Ruotolo, B. T.; Ramamoorthy, A. *J. Mol. Biol.* **2011**, *410*, 294–306.
(18) Khemtémourian, L.; Casarramona, G. L.; Suylen, D. P. L.; Hackeng, T. M.; Meeldijk, J. D.; de Kruijff, B.; Höppener, J. W. M.; Killian, J. A. *Biochemistry* **2009**, *48*, 10918–10925.
(19) Abedini, A.; Raleigh, D. P. *Biochemistry* **2005**, *44*, 16284–91.
(20) Jaikaran, E. T.; Higham, C. E.; Serpell, L. C.; Zurdo, J.; Gross, M.; Clark, A.; Fraser, P. E. *J. Mol. Biol.* **2001**, *308*, 515–25.
(21) Knight, J. D.; Miranker, A. D. *J. Mol. Biol.* **2004**, *341*, 1175–87.
(22) Rustenbeck, I.; Matthies, A.; Lenzen, S. *Lipids* **1994**, *29*, 685–92.
(23) Engel, M. F. M.; Khemtémourian, L.; Kleijer, C. C.; Meeldijk, H. J.; Jacobs, J.; Verkleij, A. J.; de Kruijff, B.; Killian, J. A.; Höppener, J. W. M. *Proc. Natl. Acad. Sci. U.S.A.* **2008**, *105*, 6033–8.
(24) Rouser, G.; Fkeischer, S.; Yamamoto, A. *Lipids* **1970**, *5*, 494–6.
(25) Davis, J. H.; Jeffrey, K. R.; Bloom, M.; Valic, M. I.; Higgs, T. P. *Chem. Phys. Lett.* **1976**, *42*, 390–394.
(26) Rance, M.; Byrd, R. A. *J. Magn. Reson.* **1983**, *52*, 221–240.
(27) Dufourc, E. J.; Mayer, C.; Stohrer, J.; Kothe, G. *J. Chim. Phys.* **1992**, *89*, 243–252.
(28) Goldsbury, C.; Goldie, K.; Pellaud, J.; Seelig, J.; Frey, P.; Muller, S. A.; Kistler, J.; Cooper, G. J.; Aebi, U. *J. Struct. Biol.* **2000**, *130*, 352–62.
(29) LeVine, H., III. *Methods Enzymol.* **1999**, *309*, 274–84.
(30) Padrick, S. B.; Miranker, A. D. *Biochemistry* **2002**, *41*, 4694–703.
(31) Khemtémourian, L.; Engel, M. F. M.; Liskamp, R. M. J.; Höppener, J. W. M.; Killian, J. A. *Biochim. Biophys. Acta* **2010**, *1798*, 1805–1811.
(32) McLaurin, J.; Chakrabartty, A. *J. Biol. Chem.* **1996**, *271*, 26482–9.
(33) Knight, J. D.; Hebda, J. A.; Miranker, A. D. *Biochemistry* **2006**, *45*, 9496–508.
(34) Demel, R. A.; London, Y.; Geurts van Kessel, W. S.; Vossenberg, F. G.; van Deenen, L. L. *Biochim. Biophys. Acta* **1973**, *311*, 507–19.
(35) Demel, R. A.; Geurts van Kessel, W. S.; Zwaal, R. F.; Roelofsen, B.; van Deenen, L. L. *Biochim. Biophys. Acta* **1975**, *406*, 97–107.
(36) Khemtémourian, L.; Engel, M. F. M.; Kruijtzer, J. A.; Höppener, J. W. M.; Liskamp, R. M. J.; Killian, J. A. *Eur. Biophys. J.* **2010**, *39*, 1359–1364.
(37) Seelig, J. *Q. Rev. Biophys.* **1977**, *10*, 353–418.
(38) Bonev, B.; Watts, A.; Bokvist, M.; Grobner, G. *Phys. Chem. Chem. Phys.* **2001**, *3*, 2904–2910.
(39) Friedman, R.; Pellarin, R.; Caflisch, A. *J. Mol. Biol.* **2009**, *387*, 407–15.
(40) Jan, A.; Adolfsson, O.; Allaman, I.; Buccarello, A. L.; Magistretti, P. J.; Pfeifer, A.; Muhs, A.; Lashuel, H. A. *J. Biol. Chem.* **2011**, *286*, 8585–96.
(41) Nanga, R. P.; Brender, J. R.; Xu, J.; Veglia, G.; Ramamoorthy, A. *Biochemistry* **2008**, *47*, 12689–97.